Supporting Information

When Push Comes to Shove: Unravelling the Mechanism and Scope of Non-Emissive *meso*-Unsaturated BODIPY Dyes

Richard Lincoln[†], Lana E. Greene[†], Cheryl Bain[†], Juan O. Flores-Rizo [†‡], D. Scott Bohle[†], and Gonzalo Cosa*[†]

[†] Department of Chemistry and Center for Self Assembled Chemical Structures, McGill University, 801 Sherbrooke Street West, Montreal, Quebec H3A 2K6, Canada.

[‡] Departamento de Química, Universidad de Guanajuato, Col. Noria Alta S/N, Guanajuato, Gto. 36050, Mexico

*To whom correspondence should be addressed:
Phone: 1 (514) 398-6932 **Fax:** 1 (514) 398-3797 **Email:** gonzalo.cosa@mcgill.ca

This section includes:

- 8-((Butylimino)Methyl)-1,3,5,7-Tetramethyl-Pyrromethene Fluoroborate (**2**) ^{1}H-NMR spectrum (page S3).
- 8-((Butylimino)Methyl)-1,3,5,7-Tetramethyl-Pyrromethene Fluoroborate (**2**) ^{13}C-NMR spectrum (page S4).
- 8-((Butylamino)Methyl)-1,3,5,7-Tetramethyl-Pyrromethene Fluoroborate (**2a**) ^{1}H-NMR spectrum (page S5).
- 8-((Butylamino)Methyl)-1,3,5,7-Tetramethyl-Pyrromethene Fluoroborate (**2a**) ^{13}C-NMR spectrum (page S6).
- 8-Vinyl-1,3,5,7-Tetramethyl-Pyrromethene Fluoroborate (**3**) ^{1}H-NMR spectrum (page S7).
- 8-Vinyl-1,3,5,7-Tetramethyl-Pyrromethene Fluoroborate (**3**) ^{13}C-NMR spectrum (page S8).
- 8-Ethyl-1,3,5,7-Tetramethyl-Pyrromethene Fluoroborate (**3a**) ^{1}H-NMR spectrum (page S9).
- 8-Ethyl-1,3,5,7-Tetramethyl-Pyrromethene Fluoroborate (**3a**) ^{13}C-NMR spectrum (page S10).
- Complete Reference 24

Gaussian 09, Revision D.01, M. J. Frisch, G. W. Trucks, H. B. Schlegel, G. E. Scuseria, M. A. Robb, J. R. Cheeseman, G. Scalmani, V. Barone, B. Mennucci, G. A. Petersson, H. Nakatsuji, M. Caricato, X. Li, H. P. Hratchian, A. F. Izmaylov, J. Bloino, G. Zheng, J. L. Sonnenberg, M. Hada, M. Ehara, K. Toyota, R. Fukuda, J. Hasegawa, M. Ishida, T. Nakajima, Y. Honda, O. Kitao, H. Nakai, T. Vreven, J. A. Montgomery, Jr., J. E. Peralta, F. Ogliaro, M. Bearpark, J. J. Heyd, E. Brothers, K. N. Kudin, V. N. Staroverov, T. Keith, R. Kobayashi, J. Normand, K. Raghavachari, A. Rendell, J. C. Burant, S. S. Iyengar, J. Tomasi, M. Cossi, N. Rega, J. M. Millam, M. Klene, J. E. Knox, J. B. Cross, V. Bakken, C. Adamo, J. Jaramillo, R. Gomperts, R. E. Stratmann, O. Yazyev, A. J. Austin, R. Cammi, C. Pomelli, J. W. Ochterski, R. L. Martin, K. Morokuma, V. G. Zakrzewski, G. A. Voth, P. Salvador, J. J. Dannenberg, S. Dapprich, A. D. Daniels, O. Farkas, J. B. Foresman, J. V. Ortiz, J. Cioslowski, and D. J. Fox, Gaussian, Inc., Wallingford CT, 2013.

- **Figure S1.** DFT-derived molecular orbitals at the B3LYP/6-31(g) level with an applied polarizable continuum model solvation of acetonitrile for compounds **1** and **2** at the ground state and excited state optimized structures. (page S11)
- **Figure S2.** Calculated energy diagram of **1** (top panel) and **2** (bottom panel) at the B3LYP/6-31g(d) level with an applied polarizable continuum model solvation of acetonitrile. Ground state (left) and excited state (right) optimized geometries shown. (page S11)
- **Figure S3.** Calculated energy diagram of 2-Formyl-1,3,5,7-Tetramethyl-Pyrromethene Fluoroborate (top-left panel), 2-Vinyl-1,3,5,7-Tetramethyl-Pyrromethene Fluoroborate (top-left panel), 3-Formyl-1,5,7-Trimethyl-Pyrromethene Fluoroborate (bottom-left panel) and 3-Vinyl-1,5,7-Trimethyl-Pyrromethene Fluoroborate (bottom-left panel) at the B3LYP/6-31g(d) level with an applied polarizable continuum model solvation of acetonitrile. Ground state (left) and excited state (right) optimized geometries shown. (page S12)

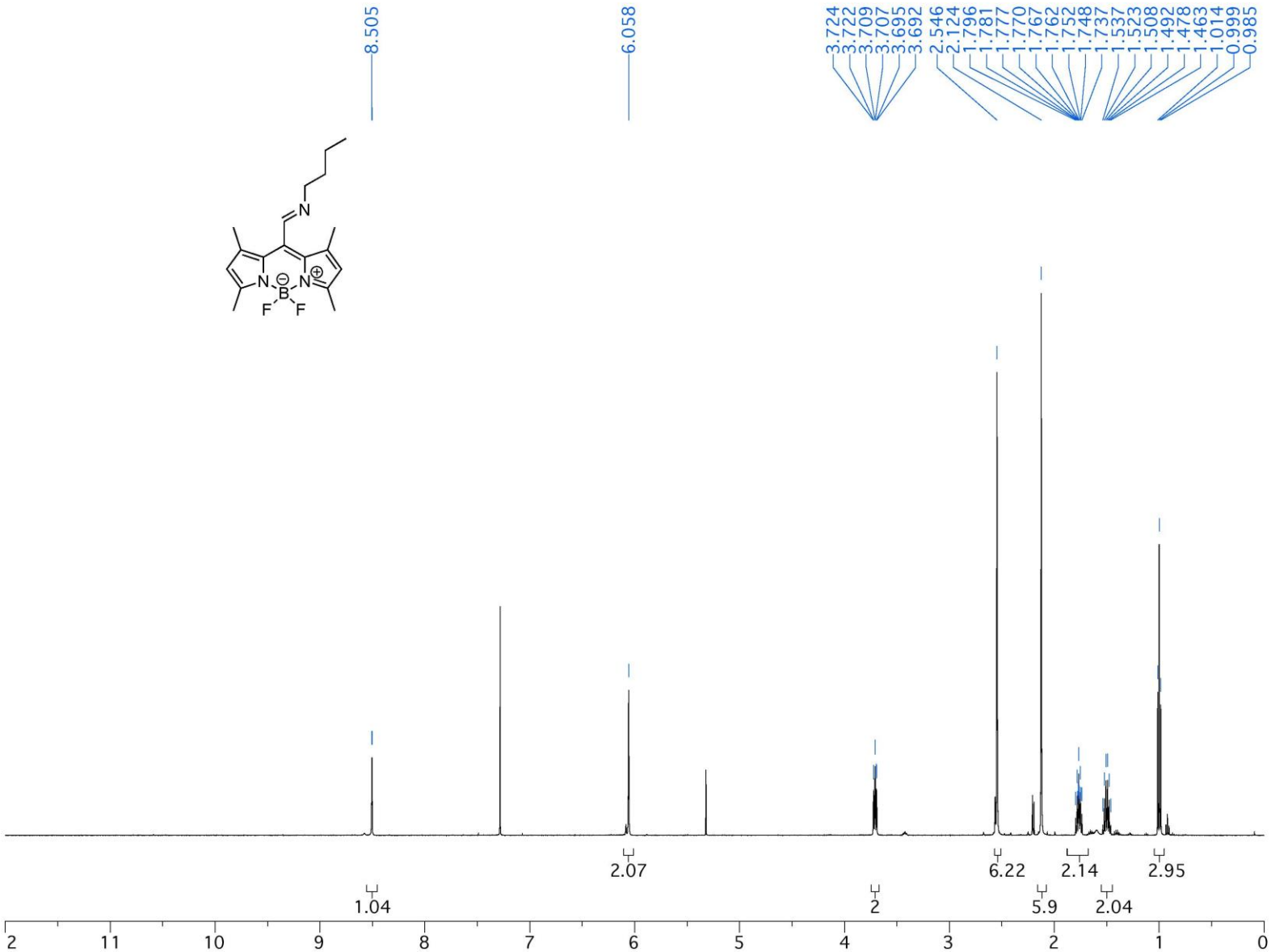
8.505
6.058
3.724
3.722
3.709
3.707
3.695
3.692
2.546
2.124
1.796
1.781
1.777
1.770
1.767
1.762
1.752
1.748
1.737
1.537
1.523
1.508
1.492
1.478
1.463
1.014
0.999
0.985
N
N
B
F
F
1.04
2.07
2
6.22
5.9
2.14
2.04
2.95
2
11
10
9
8
7
6
5
4
3
2
1
0

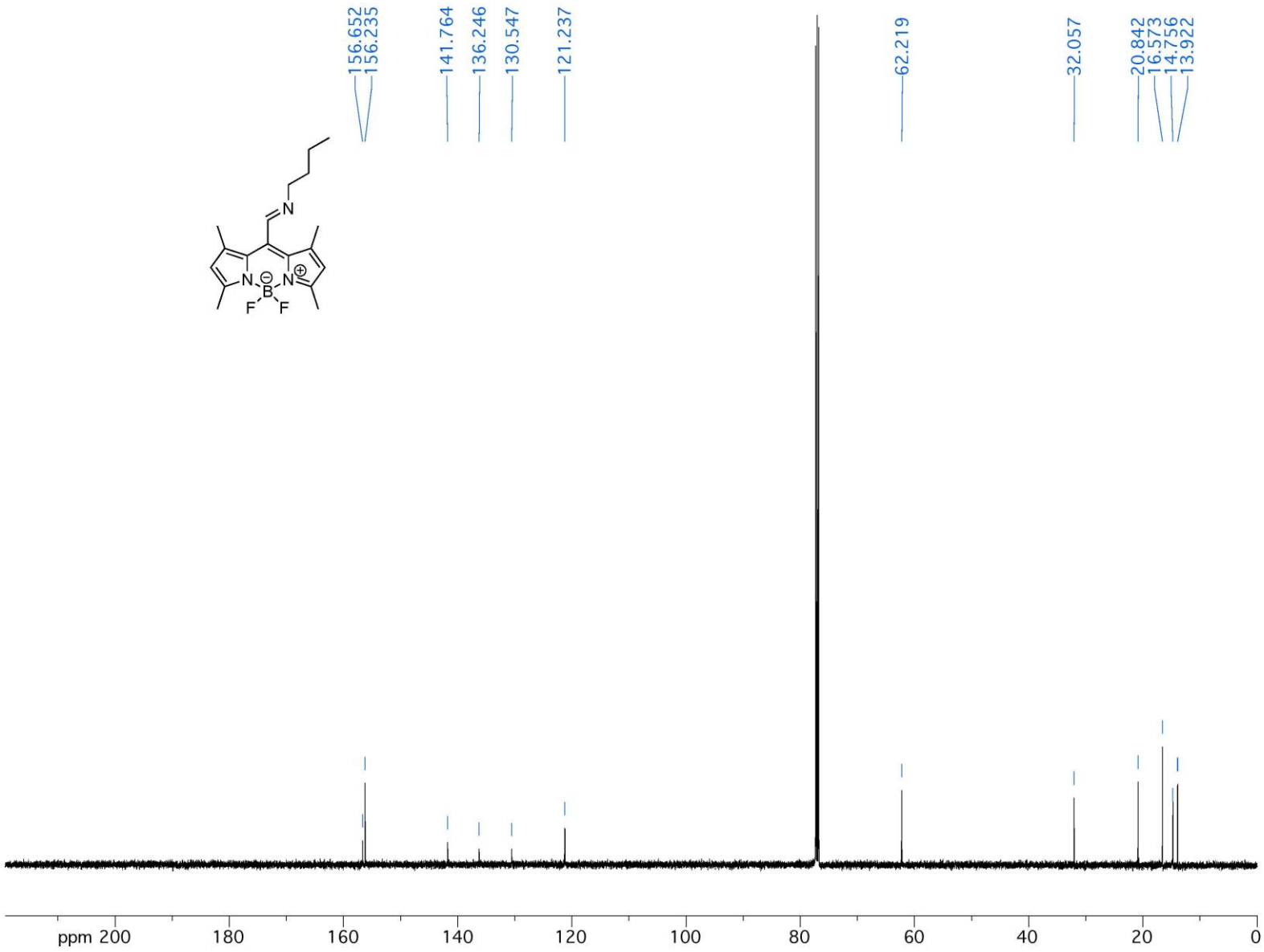
156.652
156.235
141.764
136.246
130.547
121.237
62.219
32.057
20.842
16.573
14.756
13.922
N
N
B
N
F
F
ppm 200
180
160
140
120
100
80
60
40
20
0

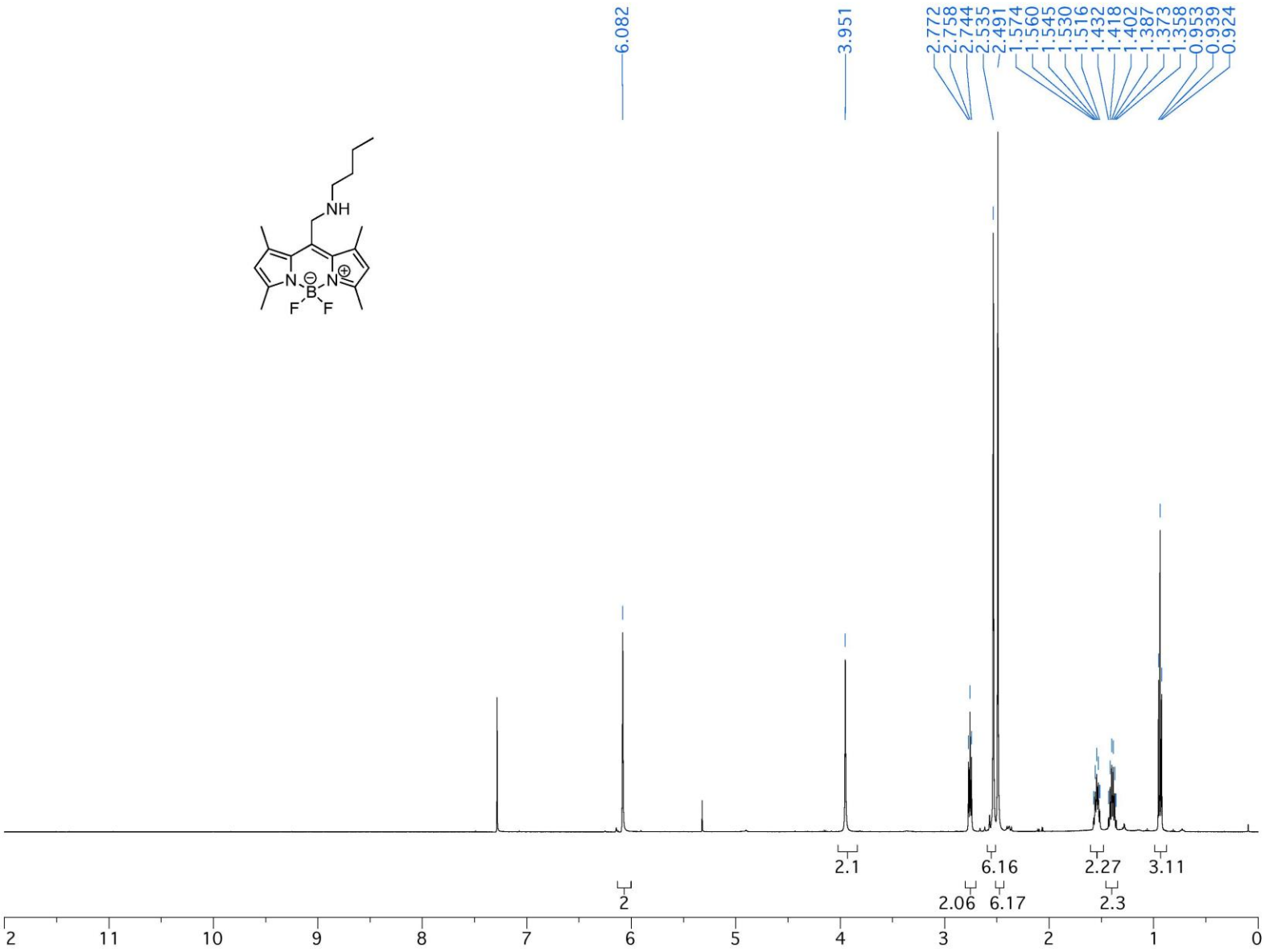
6.082
3.951
2.772
2.758
2.744
2.535
2.491
1.574
1.560
1.545
1.530
1.516
1.432
1.418
1.402
1.387
1.373
1.358
0.953
0.939
0.924
NH
N
B
N
F
F
2.1
6.16
2.27
3.11
2
2.06
6.17
2.3
2
11
10
9
8
7
6
5
4
3
2
1
0

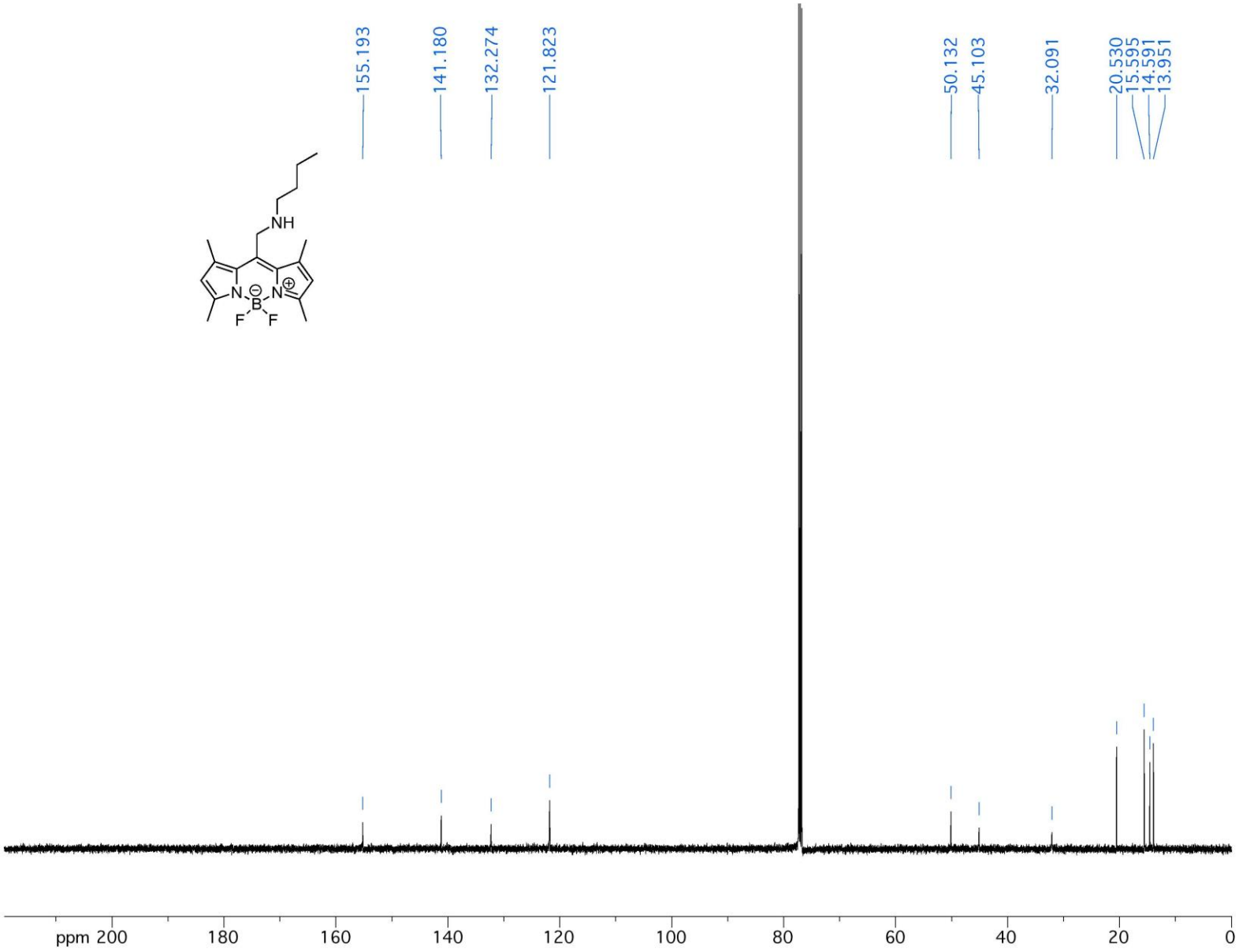
155.193
141.180
132.274
121.823
50.132
45.103
32.091
20.530
15.595
14.591
13.951
NH
N
B
N
F
F
ppm 200
180
160
140
120
100
80
60
40
20
0

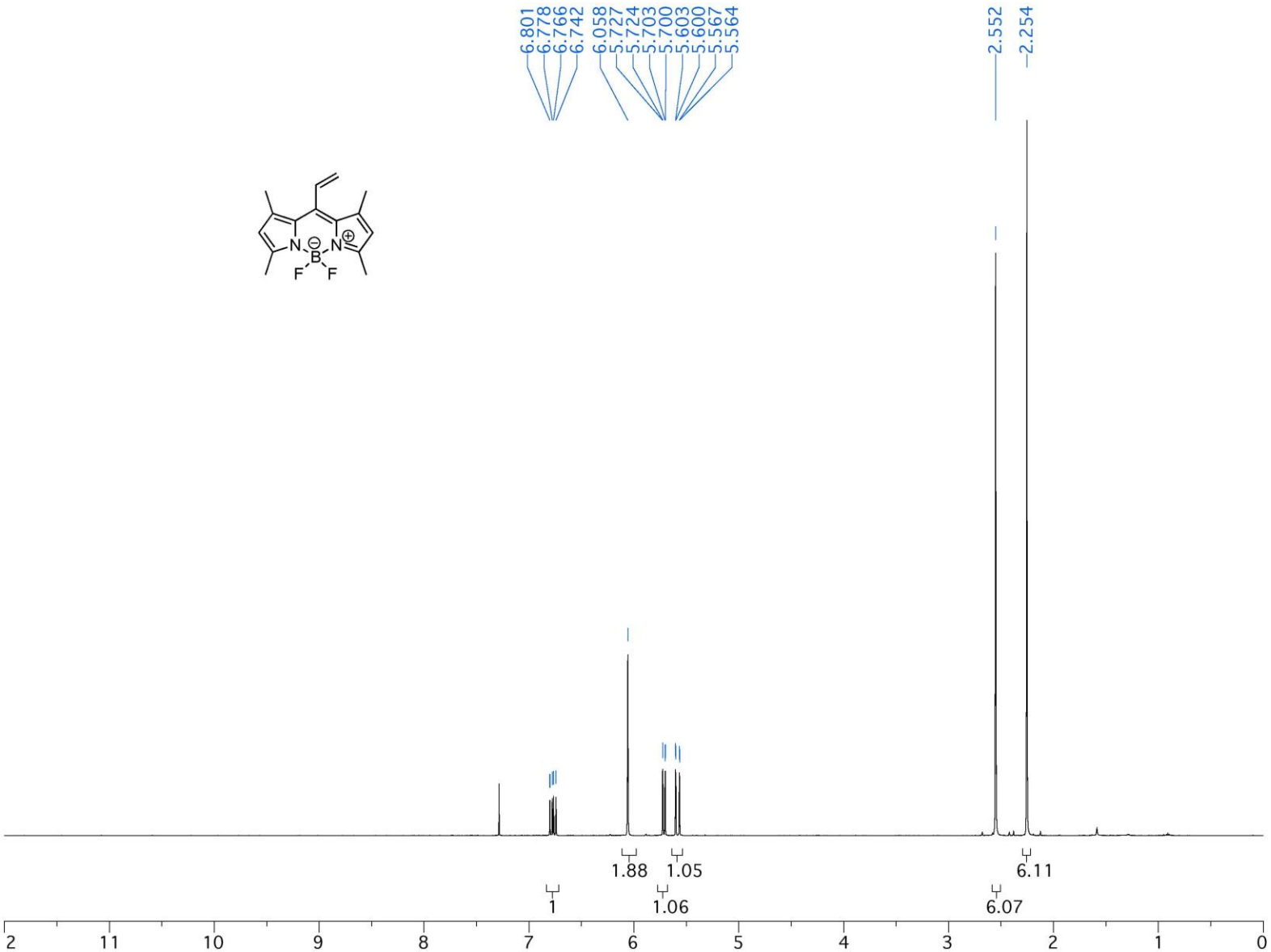
6.801
6.778
6.766
6.742
6.058
5.727
5.724
5.703
5.700
5.603
5.600
5.567
5.564
2.552
2.254
1.88
1.05
6.11
1
1.06
6.07
2
11
10
9
8
7
6
5
4
3
2
1
0

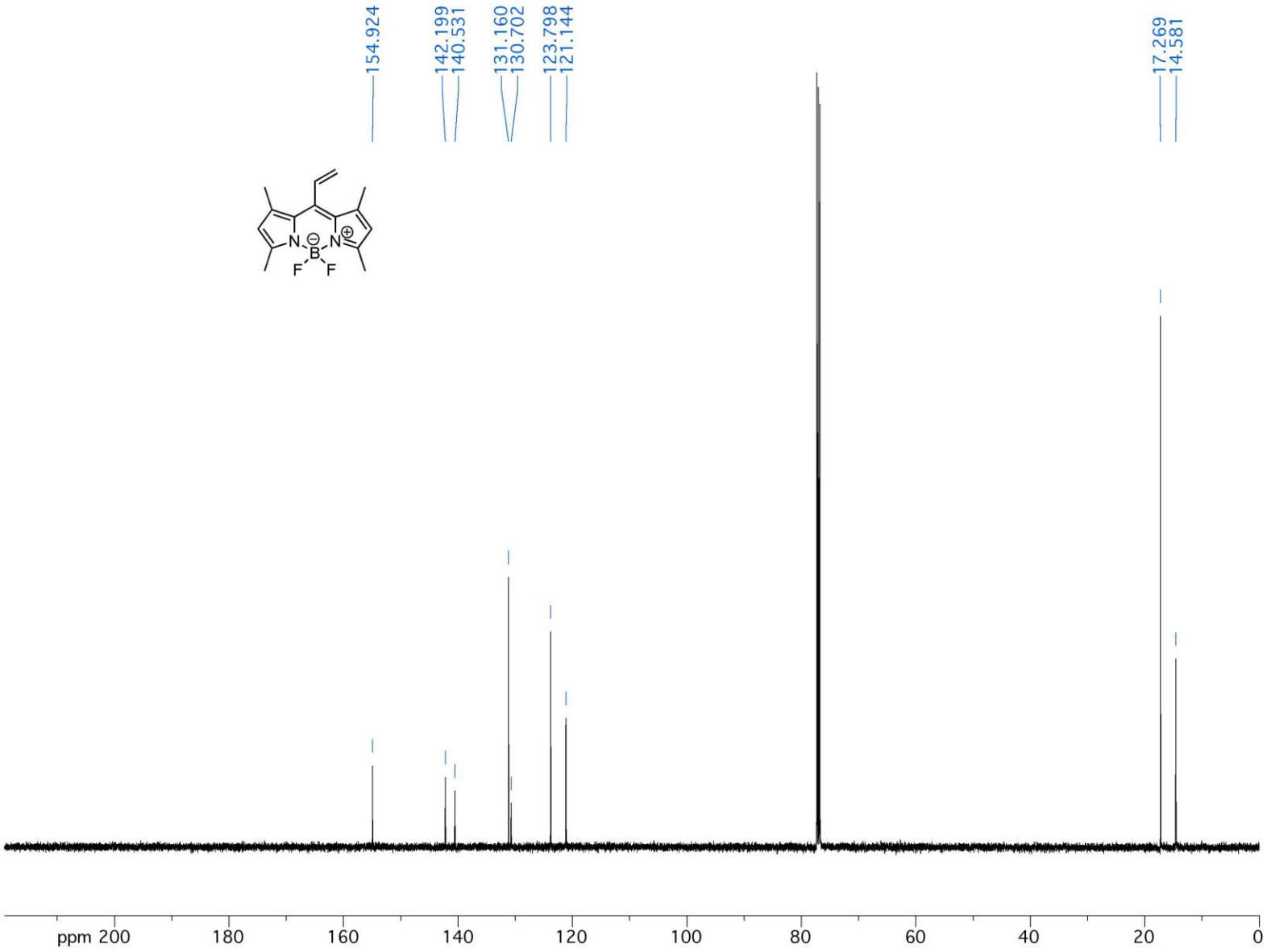
154.924
142.199
140.531
131.160
130.702
123.798
121.144
17.269
14.581
N
B
N
F
F
ppm 200
180
160
140
120
100
80
60
40
20
0

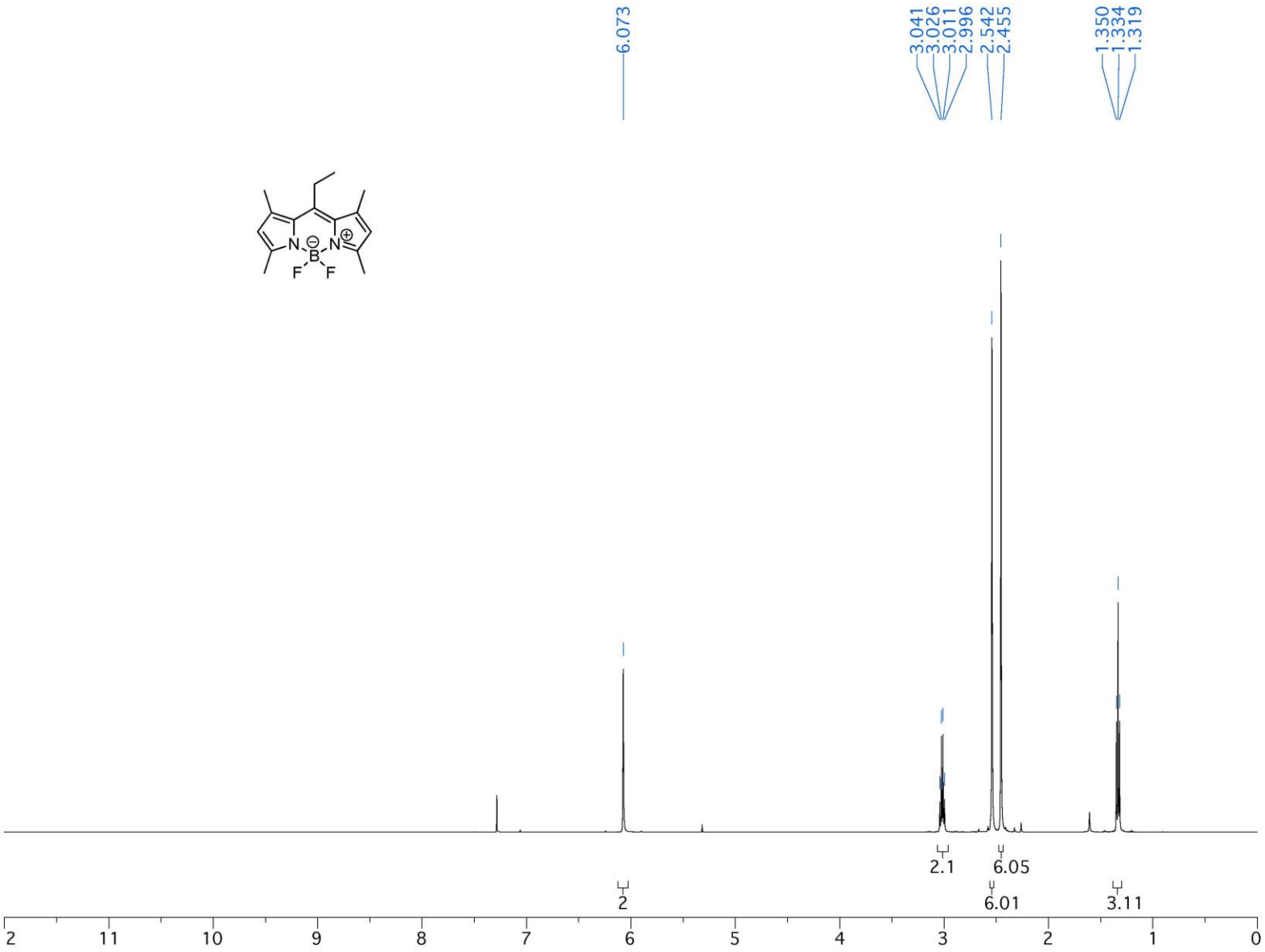
6.073
3.041
3.026
3.011
2.996
2.542
2.455
1.350
1.334
1.319
2.1
6.05
2
6.01
3.11
2
11
10
9
8
7
6
5
4
3
2
1
0

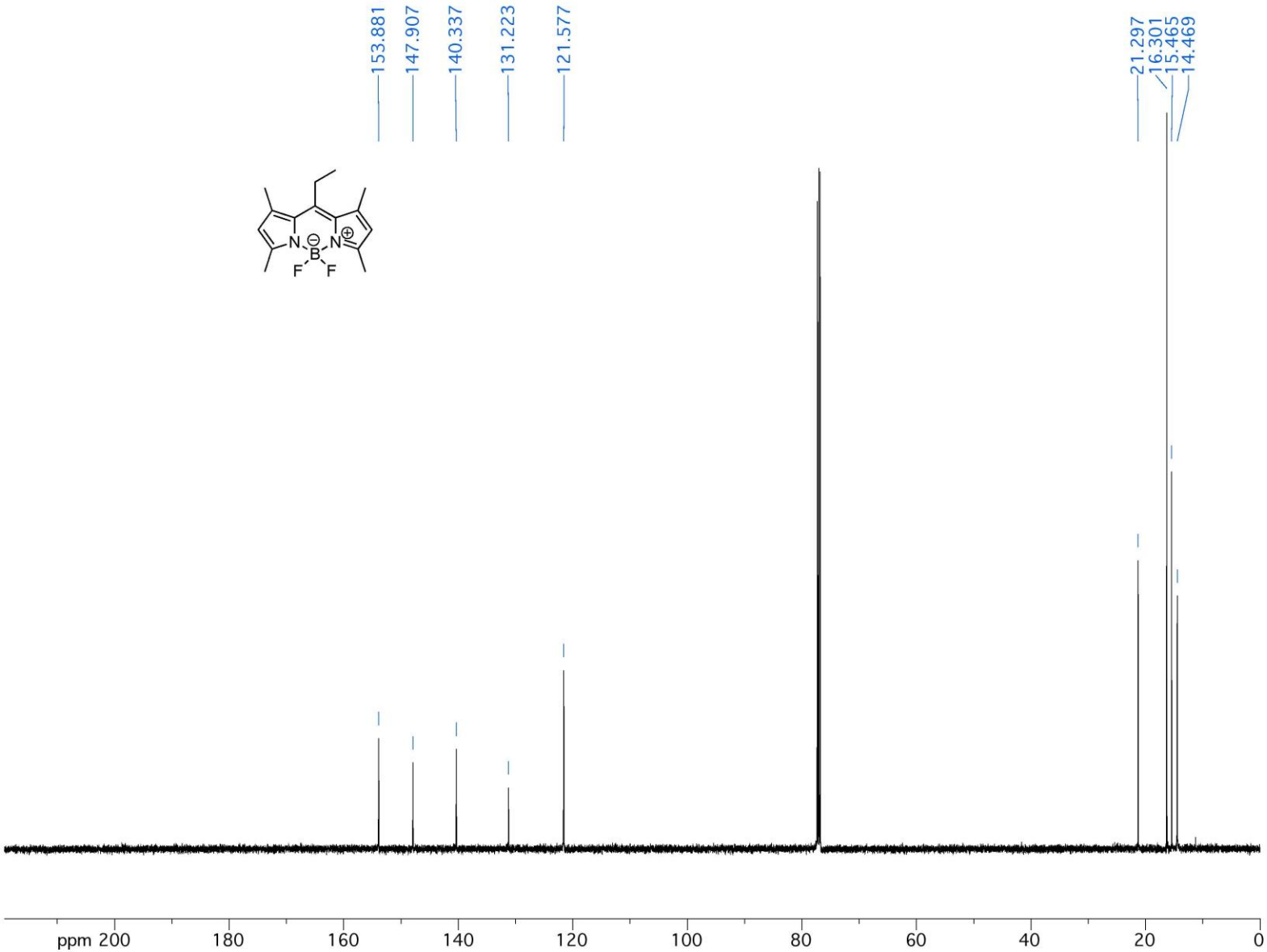
153.881
147.907
140.337
131.223
121.577
21.297
16.301
15.465
14.469
ppm 200
180
160
140
120
100
80
60
40
20
0

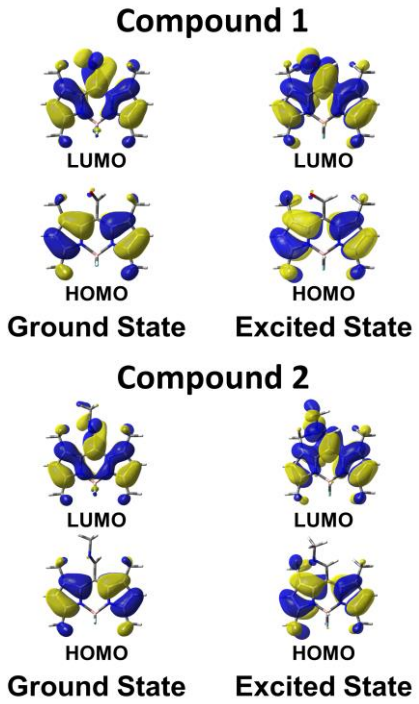

Figure S1. DFT-derived molecular orbitals at the B3LYP/6-31(g) level with an applied polarizable continuum model solvation of acetonitrile for compounds **1** and **2** at the ground state and excited state optimized structures.

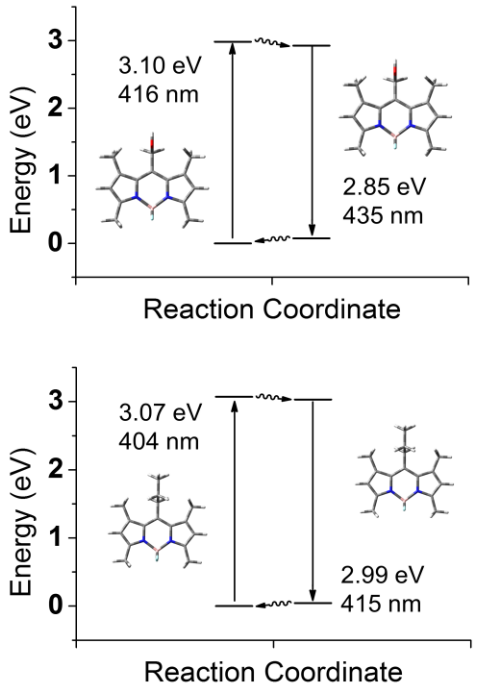

Figure S2. Calculated energy diagram of **1** (top panel) and **2** (bottom panel) at the B3LYP/6-31g(d) level with an applied polarizable continuum model solvation of acetonitrile. Ground state (left) and excited state (right) optimized geometries shown.

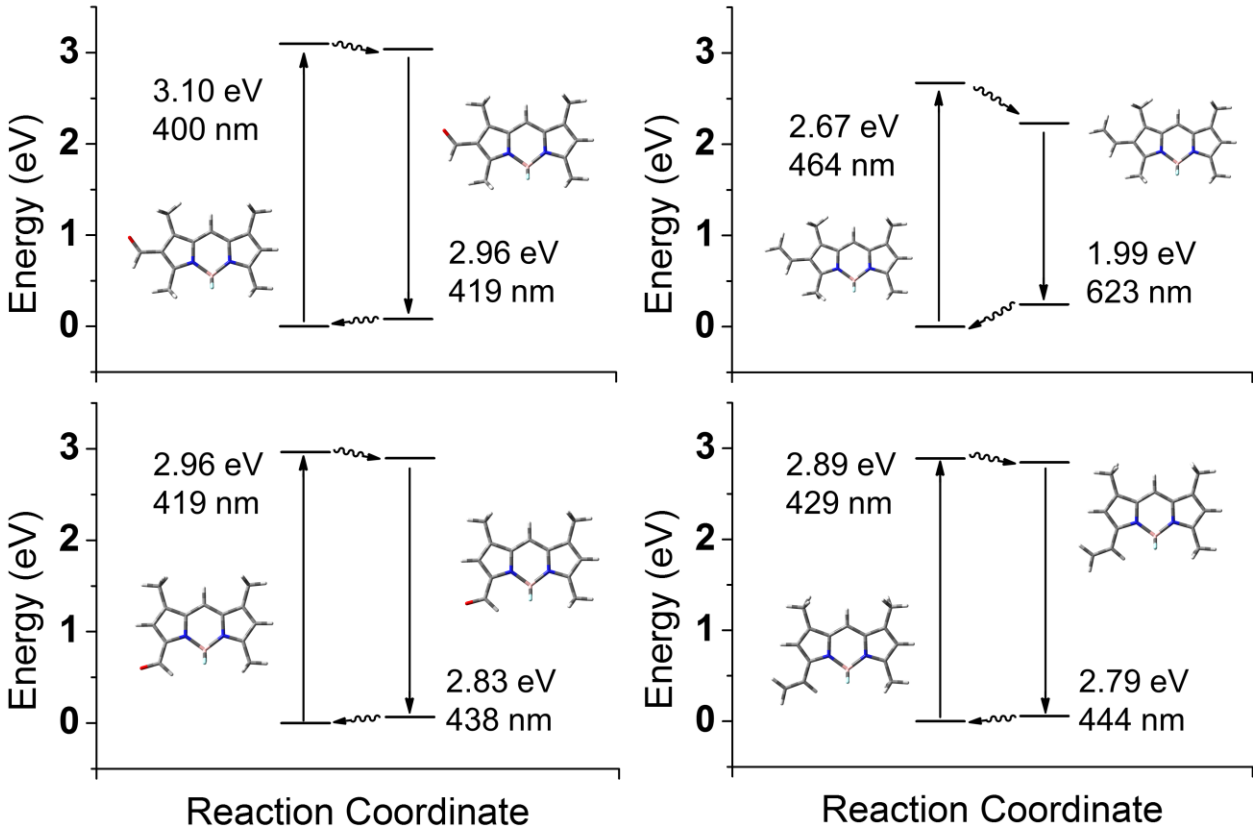

Figure S3. Calculated energy diagram of 2-Formyl-1,3,5,7-Tetramethyl-Pyrromethene Fluoroborate (top-left panel), 2-Vinyl-1,3,5,7-Tetramethyl-Pyrromethene Fluoroborate (top-left panel), 3-Formyl-1,5,7-Trimethyl-Pyrromethene Fluoroborate (bottom-left panel) and 3-Vinyl-1,5,7-Trimethyl-Pyrromethene Fluoroborate (bottom-left panel) at the B3LYP/6-31g(d) level with an applied polarizable continuum model solvation of acetonitrile. Ground state (left) and excited state (right) optimized geometries shown.